



Research article

Nonparametric multifunctional GARCH time series data analysis: Application to dynamic forecasting in financial data

Ali Laksaci¹, Fatimah Alshahrani², Ibrahim M. Almanjahie^{1,*} and Zoulikha Kaid¹

¹ Department of Mathematics, College of Science, King Khalid University, Abha 62223, Saudi Arabia

² Department of Mathematical Sciences, College of Science, Princess Nourah bint Abdulrahman University, P.O. Box 84428, Riyadh 11671, Saudi Arabia

* **Correspondence:** Email: imalmanjahi@kku.edu.sa.

Abstract: Financial risk management using the generalized autoregressive conditional heteroskedasticity model is a primordial topic in financial data analysis. It helps to improve risk assessment accuracy by taking into account the time-varying volatility. In this paper, we improved this feature by analyzing the functional nature of the high-frequency financial data. Specifically, we investigated the nonparametric estimation method of the multifunctional expectile function based on a kernel technique, developed the estimator, and established its stochastic consistency. The obtained asymptotic result provided a good mathematical foundation allowing us to enhance the expectile applicability in financial risk analysis. We assessed the algorithm's efficiency through empirical testing, and illustrated the practical value of expectile estimation in multi-asset risk management by applying it to real-world financial data with diverse scenarios.

Keywords: asymmetric error; expectile regression; value at risk; functional data; coherent measures; expected shortfall; risk management; prediction markets; big data analysis

Mathematics Subject Classification: 62G05, 62G08, 62R20

1. Introduction

The swift and the current technological progression have accelerated the digital transformation of the financial system. In this context, real-time monitoring and management of market volatility become imperative. Therefore, conventional multivariate parametric statistical tools are inadequate for addressing this challenge. Alternatively, in this study, we introduce a novel data-driven framework designed to manage multiple financial risks dynamically. Our approach is based on a real-time risk assessment with a specific focus on quantifying market risk through expectiles estimation using

multi-functional covariate regression.

Often the financial volatility plays a pivotal role in investment decision-making. Thus, providing a dynamic and robust model to fit the rough volatility is fundamental for financial risk assessment. The former topic has been widely explored in the field of statistical and financial literature through some specific time series models. In particular, the pioneer result on this topic was established by [1]. The author explored the implications of the autoregressive conditional heteroscedasticity (ARCH) model. The issues were generalized in [2] within the Generalized Autoregressive Conditional Heteroskedasticity (GARCH) framework. They introduced a functional variant of the GARCH model, demonstrating estimator consistency and providing prerequisites for the existence of a strictly stationary solution. We cite [3] for an illustrative application of the functional GARCH in modeling high-frequency data. Meanwhile, [4] proposed a quasi-likelihood-based alternative estimation method, establishing the asymptotic normality of their estimator. Readers interested in recent deeper analysis in functional GARCH time series may consult [5,6] and the references therein. In parallel, it is well recommended that the expectile model constitutes a good alternative financial risk model than the Value-at-Risk (VaR) and the expected shortfall. It permits us to correct some drawbacks in these conventional models, namely the non-coherence and the non-elicability.

In fact, the nonfunctional expectile model has been extensively studied in mathematical statistics. For an early parametric approach, we mention the work in [7] that explored the behavior of the asymptotic multivariate expectiles for the Fréchet model. This cited reference established an estimator for the extreme values using the expectile function. [8] demonstrated that expectiles offer a good alternative to the VaR and expected shortfall; particularly, due to their high sensitivity to outlier observations. In applied fields like econometrics, finance, and actuarial science, the dynamic expectile regression has gained traction—pioneered by [9] and further developed in [10]. The theoretical properties of the dynamic expectiles have been widely developed in vectorial statistics. For instance, [11] generalized conditional expectations to conditional expectiles via asymmetric quadratic loss minimization, while [12] and [13] laid the groundwork for regression quantile estimation using asymmetric loss functions. Recently, [14] employed expectiles to estimate the VaR and expected shortfall. Additional contributions on dynamic expectile modeling can be found in [15–18], with [17], specifically, extending the framework to multivariate risk measures and analyzing their coherence properties. Despite these advances, existing literature primarily addresses finite-dimensional settings. Our work diverges by examining the influence of a functional-covariate on a scalar-response—a problem first tackled by [19], who established almost complete convergence and asymptotic normality for the Nadaraya-Watson estimator under independence. Subsequent work in [20] generalized these results to dependent data, while [21] introduced a functional local linear estimator with Borel-Cantelli convergence guarantees.

Furthermore, recent years have seen significant progress in risk management methodologies, particularly in the development of GARCH frameworks. We refer to [22] for the use of the VaR function, [23] for the asymmetric GARCH framework case, or [24] for the multifunctional GARCH model. While existing literature primarily relies on the VaR for financial risk forecasting, this study introduces a dynamic expectile-based approach. The primary innovation lies in analyzing multi-asset financial movements through their continuous historical price trajectories, enabling real-time monitoring of their volatility. Mathematically, we develop a nonparametric estimator for this model by employing the functional extension of the Nadaraya-Watson estimator. Beyond estimation, we

derive its asymptotic properties, specifically, quantifying the convergence rate to establish almost complete consistency. The obtained results are stated under multi-functional GARCH structure. Undoubtedly, the multivariate functional GARCH time series model is a common structure in applied fields, particularly in finance, in which it controls the possible interactions between several portfolio trajectories. This approach is especially valuable for analyzing dynamic dependencies in financial markets, where interconnections among diverse assets are inevitable and have great impact on the financial market behavior. Finally, note that the integration of the GARCH framework with multifunctional modeling plays a critical role in financial risk analysis. This approach enhances prediction accuracy by systematically controlling the complex interdependencies among financial variables, thereby improving the assessment of market fluctuations. To evaluate this gain, we conducted an empirical analysis using both artificially generated data and real-world datasets, ensuring comprehensive validation of the proposed algorithm. To our knowledge, the literature currently available does not address this particular problem, which has prompted our current investigation to advance understanding in this domain.

We organize the paper as follows. Section 2 introduces the framework of our functional statistics and outlines the motivations behind this study. In Section 3, we present the main theoretical results, establishing the foundation for our analysis. Section 4 provides an empirical investigation, including illustrative examples that highlight various aspects of multivariate functional generalized ARCH (MFGARCH) models. Section 5 details an example of an application using real data. It permits us to assess the practical relevance of our approach. Finally, the conclusion is presented in Section 6. The Appendix contains the technical derivations and proofs of intermediate results.

2. Multivariate functional GARCH framework

Let $\{V_i(t)\}_{i=1}^n$ denote n -days portfolio price trajectories, each consisting of m financial assets, where t represents continuous time. We model these trajectories as a multi-functional process, where each $V_i(t)$ is an m -dimensional vector,

$$V_i(\cdot) = \begin{pmatrix} V_i^1(\cdot) \\ V_i^2(\cdot) \\ \vdots \\ V_i^m(\cdot) \end{pmatrix}, \quad i = 1, \dots, n.$$

It is well documented that the financial risk assessment aims to forecast the fluctuations in future characteristics of the process $V(\cdot)$. Commonly, these characteristics are represented by fixed real valued metrics such as closing prices, maximum values, values at a specific time t_0 , or variations over a given interval frame. To formalize this problem, we model the future characteristics of interest as the response variable $(U_i)_{i=1, \dots, n}$, represented as

$$U_i = F u(V_i), \quad i = 1, \dots, n. \quad (1)$$

At this stage, financial risk assessment is conducted through the analysis of functional observations, $O_i = (V_i, U_i)_{i=1, \dots, n}$. Precisely, we utilize a dynamic expectile function to provide a dynamic and data-driven evaluation of potential vulnerabilities in portfolio price. Formally, we

assume that $O_i = (V_i, U_i)_{i=1,\dots,n}$ are defined in probability space, $(\Omega, \mathfrak{F}, P)$ and valued in the field $\mathcal{F} \times \mathbb{R}$, where the former represents the product of m semi-metric space \mathcal{F}^j , i.e., $\mathcal{F} = \underbrace{\mathcal{F}^1 \times \mathcal{F}^2 \dots \times \mathcal{F}^m}_{m\text{-time}}$. Note that \mathcal{F}^j is equipped with a semi-metric d_j . In addition, the vector

$\mathbf{V} = \begin{pmatrix} \mathbf{V}^1 \\ \mathbf{V}^2 \\ \vdots \\ \mathbf{V}^m \end{pmatrix} \in \mathcal{F}$, and we use $\mathcal{N}_{\mathbf{V}}$ to represent the given neighborhood of \mathbf{V} , which is represented by

the metric d on \mathcal{F} with $d(\cdot, \cdot) = \sum_{j=1}^m d_j(\cdot, \cdot)$. Now, for $0 < \tau < 1$, we define the dynamic expectile $DE_{\tau}(\mathbf{V})$ of order τ as the unique solution with respect to (w.r.t.) s of the following optimization problem:

$$\min_{s \in \mathbb{R}} \left\{ \mathbb{E} \left[\tau(U - s)^2 \mathbb{1}_{(U-s)>0} \mid V = \mathbf{V} \right] + \mathbb{E} \left[(1 - \tau)(U - s)^2 \mathbb{1}_{(U-s)\leq 0} \mid V = \mathbf{V} \right] \right\}, \quad (2)$$

where $\mathbb{1}_A$ denotes the indicator function of the set A . Analytically, we prove that $DE_{\tau}(\mathbf{V})$ is the unique solution w.r.t. s of

$$DE_{\tau}(\mathbf{V}) = \arg \min \left\{ s \in \mathbb{R} : L(s; \mathbf{V}) \geq \frac{\tau}{1 - \tau} \right\} \quad (3)$$

where

$$L(s; \mathbf{V}) := \frac{-\mathbb{E} [(U - s) \mathbb{1}_{(U-s)\leq 0} \mid V = \mathbf{V}]}{\mathbb{E} [(U - s) \mathbb{1}_{(U-s)>0} \mid V = \mathbf{V}]} \quad (4)$$

In the financial area, the dynamic expectile serves as a meaningful threshold, quantifying the trade-off between profit and loss functions. This interpretation allows investors to assess risk with more prudence. Thereafter, we estimate the risk detector $DE_{\tau}(\mathbf{V})$ as the solution of

$$\widehat{DE}_{\tau}(\mathbf{V}) = \arg \min \left\{ s \in \mathbb{R} : \widehat{L}(s; \mathbf{V}) \geq \frac{\tau}{1 - \tau} \right\}, \quad (5)$$

where

$$\widehat{L}(s; \mathbf{V}) = \frac{-\sum_{i=1}^n \prod_{j=1}^m \mathfrak{L}(b_n^{-1} d_j(\mathbf{V}^j, V_i^j))(U_i - s) \mathbb{1}_{(U_i-s)\leq 0}}{\sum_{i=1}^n \prod_{j=1}^m \mathfrak{L}(b_n^{-1} d_j(\mathbf{V}^j, V_i^j))(U_i - s) \mathbb{1}_{(U_i-s)>0}}, \quad \text{for } s \in \mathbb{R}, \quad (6)$$

where \mathfrak{L} is a kernel function and b_n is a sequence of positive real numbers that converges to zero as n approaches infinity.

In order to emphasize the role of the time-varying of the volatility, we assume that the vectors $V_i(t)$ are sampled from multivariate functional GARCH process. Precisely, we consider a functional version of GARCH based on the dynamic conditional correlation, presented in [25], for which the functional regressors are

$$V_i = \mathbf{H}_i^{1/2} \odot \Xi_i, \quad i = 1, \dots, n, \quad (7)$$

where \odot represents the pointwise product, Ξ_i denotes a vector of independent functional random variables, and \mathbf{H}_i represents the conditional covariance matrix that can be, with volatility, decomposed by

$$\mathbf{H}_i = \mathbf{D}_i \mathbf{R}_i \mathbf{D}_i, \quad i = 1, \dots, n,$$

with \mathbf{R}_i denoting the correlation matrix based on a continuous time-varying and \mathbf{D}_i a diagonal matrix with functional structure, defined by

$$\mathbf{D}_i = \begin{pmatrix} \lambda_i^1 & \dots & \dots & 0 \\ 0 & \lambda_i^2 & \dots & 0 \\ \vdots & \vdots & \ddots & \vdots \\ 0 & \dots & \dots & \lambda_i^m \end{pmatrix}.$$

The diagonal is

$$\begin{pmatrix} \lambda_i^1 \\ \lambda_i^2 \\ \vdots \\ \lambda_i^m \end{pmatrix} = \begin{pmatrix} w^1 \\ w^2 \\ \vdots \\ w^m \end{pmatrix} + \sum_{k=1}^p \alpha_k \begin{pmatrix} V_{i-k}^{1^2} \\ V_{i-k}^{2^2} \\ \vdots \\ V_{i-k}^{m^2} \end{pmatrix} + \sum_{j=1}^q \beta_j \begin{pmatrix} \lambda_{i-j}^1 \\ \lambda_{i-j}^2 \\ \vdots \\ \lambda_{i-j}^m \end{pmatrix}.$$

Note that $(\alpha_k)_k$ and $(\beta_j)_j$ represent the linear operators. In a multivariate context, these formulations extend the univariate functional GARCH process, which was initially presented in [7]. We may use it to emphasize the time-varying character of covariances and correlations between several assets in a continuous-time environment. Based on the MFGARCH model and similar to [7], the ergodicity and strict stationarity are related to the Lyapunov exponent of a sequence of matrix operators, defined by

$$\Phi_k^{(p,q)} = \begin{pmatrix} \otimes_k \alpha_1 & \dots & \otimes_k \alpha_p & \otimes_k \beta_1 & \dots & \otimes_k \beta_{q-1} & \otimes_k \beta_q \\ I & \dots & 0 & 0 & \dots & 0 & 0 \\ \vdots & \vdots & \vdots & \vdots & \vdots & \vdots & \vdots \\ 0 & \dots & I & 0 & \dots & 0 & 0 \\ \alpha_1 & \dots & \alpha_p & \beta_1 & \dots & \beta_{q-1} & \beta_q \\ 0 & \dots & 0 & I & \dots & 0 & 0 \\ \vdots & \vdots & \vdots & \vdots & \vdots & \vdots & \vdots \\ 0 & \dots & 0 & I & \dots & 0 & 0 \\ \vdots & \vdots & \vdots & \vdots & \vdots & \vdots & \vdots \\ 0 & \dots & 0 & 0 & \dots & I & 0 \end{pmatrix}.$$

Here, \otimes_k denotes the operator mapping, where $\otimes_k(\mathcal{X}) := \mathcal{X} \odot \Xi_k^2$. In this paper, we assume that:

DE1. The top Lyapunov exponent of the sequence $\Phi_k^{(p,q)}$ is

$$\gamma^{(p,q)} = \lim_{k \rightarrow \infty} \mathbb{E} \log \|\Phi_k^{(p,q)} \Phi_{k-1}^{(p,q)} \dots \Phi_1^{(p,q)}\| < 0,$$

with $\|\cdot\|$ denoting the norm over a functional matrix with order $p + q$. Readers can check [26] for more discussion on this assumption and its variations. Let us point out that the functional GARCH process is a new model in time series data analysis, first introduced in [4]. More generally, in this work, we focus on the multifunctional case, which is recent development by [7]. This new model constitutes an alternative approach to standard continuous-time (CT) processes, such as the COGARCH and Lévy processes. Indeed, unlike traditional models that treat (in practice) the continuous-time (CT) model by considering only discrete grid points of the trajectories, the functional GARCH model fits the CT

model by considering the entire trajectory as a continuous curve in a functional space. Furthermore, the functional GARCH model combines the advantages of both the GARCH process and functional data analysis. In particular, the GARCH model is well known for its ability to model the high variability of volatility, which is essential for financial applications, namely, for financial risk management. In parallel, functional statistics are a the modern branch of statistics that offer powerful tools for analyzing data that vary continuously over time or space. Therefore, combining these two approaches is highly beneficial in practice, as it allows us to explore the dynamic and time-varying nature of volatility in a fast manner. We refer the reader to [4] and [7] for more motivation and deeper discussion on the functional GARCH model.

Recall that our aim in this paper is to establish the almost complete convergence (a.co.). This is stronger than the almost surely or the probability consistencies. In fact, we say that the sequence $(Z_n)_n$ converges a.co. to zero, if and only if

$$\forall c > 0, \sum_{n \geq 1} \mathbb{P}(|Z_n| > c) < \infty.$$

Furthermore, we say that $Z_n = O_{a.co.}(s_n)$ if there exists $c_0 > 0$ such that

$$\sum_{n \geq 1} \mathbb{P}(|Z_n| > c_0 s_n) < \infty$$

of $\widehat{DE}_\tau(\mathbf{V})$ to $DE_\tau(\mathbf{V})$.

3. Notations, postulates and results

Before proceeding to state the claimed consistency, we start by introducing some strictly positive constants C, C' . For $b > 0$, we consider a ball defined by

$$B(\mathbf{V}, b) := \left\{ \mathbf{V}' \in \mathcal{F} / d(\mathbf{V}', \mathbf{V}) = \sum_{j=1}^m d_j(\mathbf{V}'^j, \mathbf{V}^j) < b \right\}.$$

Moreover, we set

$$L_1(s; \mathbf{V}) := \mathbb{E} [(U - s) \mathbb{1}_{(U-s) \leq 0} \mid V = \mathbf{V}],$$

and

$$L_2(s; \mathbf{V}) := \mathbb{E} [(U - s) \mathbb{1}_{(U-s) > 0} \mid V = \mathbf{V}].$$

Furthermore, for $i = 1, \dots, n$, \mathfrak{F}_i is taken as the σ -algebra generated by $((V_1, U_1), \dots, (V_i, U_i))$ and \mathfrak{G}_i as the σ -algebra generated by $((V_1, U_1), \dots, (V_i, U_i), V_{i+1})$. Hence, the below hypotheses are assumed:

DE2. The processes $(V_i, U_i)_{k \in \mathbb{N}}$ satisfy:

$$\left\{ \begin{array}{l} \text{(i) The function } \mathfrak{B}(m, \mathbf{V}, b) := \mathbb{P}(P \in B(\mathbf{V}, b)) > 0, \quad \forall b > 0. \\ \text{(ii) For all } i = 1, \dots, n, \text{ there exists a deterministic function } \mathfrak{B}_i(m, \mathbf{V}, \cdot) \text{ such that} \\ \quad 0 < \mathbb{P}(V_i \in B(\mathbf{V}, b) \mid \mathfrak{F}_{i-1}) \leq \mathfrak{B}_i(m, \mathbf{V}, b), \quad \forall r > 0. \\ \text{(iii) For all } b > 0, \frac{1}{n \mathfrak{B}(m, \mathbf{V}, b)} \sum_{i=1}^n \mathbb{P}(V_i \in B(\mathbf{V}, b) \mid \mathfrak{F}_{i-1}) \rightarrow 1 \quad a.co. \end{array} \right.$$

DE3. The function $L_{i=1,2}(\cdot; \mathbf{V})$ is differentiable in \mathbb{R} and satisfies the following (Lipschitz) condition: $\exists a > 0, \forall s \in [DE_\tau(\mathbf{V}) - a, DE_\tau(\mathbf{V}) + a], \forall \mathbf{V}_1, \mathbf{V}_2 \in \mathcal{F}$,

$$|L_i(s; \mathbf{V}_1) - L_i(s; \mathbf{V}_2)| \leq C_i d^{k_i}(\mathbf{V}_1, \mathbf{V}_2) \text{ for } k_i > 0 \text{ for } i = 1, 2.$$

Furthermore, we assume that $\forall \mathbf{V} \in \mathcal{F}, L'_i(DE_\tau(\mathbf{V}); \mathbf{V})$ are not identical to zero, with $L'_i(\cdot; \mathbf{V})$ denoting the derivative of the function $L_i(\cdot; \mathbf{V})$ with respect to t .

DE4. For each $q \geq 2$, $\mathbb{E} \left[|U_i^-|^q \mid V = \mathbf{V} \right] \leq C_3 < \infty$, with $U_i^- = (U_i - s) \mathbb{1}_{(U_i-s) \leq 0}$.

DE5. There exists $\delta > 3$ such that

$$\lim_{n \rightarrow \infty} \frac{\mathfrak{A}(m, \mathbf{V}, b_n) \log n}{n^2 \mathfrak{B}^2(m, \mathbf{V}, b_n)} = 0 \quad \text{and} \quad \frac{n^{2\delta/q-1} \log n}{\mathfrak{A}(m, \mathbf{V}, b_n)} \rightarrow \infty,$$

where $\mathfrak{A}(m, \mathbf{V}, b_n) = \sum_{i=1}^n \mathfrak{B}_i(m, \mathbf{V}, b_n)$ and $\delta > q + 1$.

DE6. $\mathfrak{L}(\cdot)$ is a function with support $(0, 1)$ such that

$$0 < C \mathbb{1}_{(0,1)} < \mathfrak{L}(t) < C' \mathbb{1}_{(0,1)} < \infty.$$

DB1. The function

$$L(s; \mathbf{V}) := \mathbb{E} \left[(U - s)^2 \mid V = \mathbf{V} \right]$$

is differentiable with respect to s and satisfies the following Lipschitz condition: $\exists a > 0, \forall s \in [DE_\tau(\mathbf{V}) - a, DE_\tau(\mathbf{V}) + a], \forall \mathbf{V}_1, \mathbf{V}_2 \in \mathcal{F}$,

$$|L(s; \mathbf{V}_1) - L(s; \mathbf{V}_2)| \leq C d^r(\mathbf{V}_1, \mathbf{V}_2), \text{ for } r > 0.$$

DB2. The function $\mathfrak{L}(\cdot)$ satisfies **(DE6)** and is differentiable on $(0, 1)$ with derivative $\mathfrak{L}'(\cdot)$ such that

$$C \mathbb{1}_{(0,1)}(\cdot) \leq \mathfrak{L}'(\cdot) \leq C \mathbb{1}_{(0,1)}(\cdot).$$

DB3. The concentration property given in **(DE2)** holds and there exists a function $\beta_{\mathbf{V}}(\cdot)$ such that

$$\forall s \in [0, 1], \text{ such that } \lim_{h \rightarrow 0} \frac{\mathfrak{B}(m, \mathbf{V}, sh)}{\mathfrak{B}(m, \mathbf{V}, h)} = \beta_{\mathbf{V}}(s),$$

$$B_1 = \mathfrak{L}(1) - \int_0^1 (\mathfrak{L}'(s) \beta_{\mathbf{V}}(s)) ds \neq 0 \text{ and } B_2 = \mathfrak{L}^2(1) - \int_0^1 (\mathfrak{L}'(s) \beta_{\mathbf{V}}(s))^2 ds > 0.$$

Comments on the hypotheses

These conditions are relatively mild and align with standard frameworks in nonparametric functional statistics. Such conventional assumptions, mirroring the structural foundations, are outlined in [27]. These assumptions permit us to cover numerous classes of financial time series data. In particular, the multivariate functional GARCH model together with Dynamic Conditional Correlation (DCC) plays a pivotal role in financial econometrics. It fits time-varying correlations across multiple assets, which are necessary feature for management and portfolio optimization. Examining the functional properties of this process is particularly insightful, as it reveals structural

dependencies without imposing overly restrictive assumptions. Specifically, condition **DE2** ensures the ergodicity of the functional data, offering a more flexible framework than that mentioned in [8]. Unlike [8], **DE2** does not require decomposing concentration functions, thereby eliminating the need for the Onsager-Machlup function [28]. Hypothesis **DE3** serves as a regularity condition that defines our functional space model, ensuring that we can properly compute the bias in our asymptotic findings. Meanwhile, conditions in **DE4**, **DE5**, and **DE6** are technical assumptions and comparable to those used in prior work [27], and help establishing the necessary theoretical framework for our analysis. The additional conditions **DB1–DB3** are needed for the asymptotic normality result. They are standard and represent a modified version of the initial conditions.

The theorem below presents our main finding.

Theorem 3.1. *Consider that **DE1–DE6** are satisfied. Then, we have*

$$\widehat{DE}_\tau(\mathbf{V}) - DE_\tau(\mathbf{V}) = O\left(b_n^{\min(k_1, k_2)}\right) + O\left(\sqrt{\frac{\mathfrak{A}(m, \mathbf{V}, b_n) \log n}{n^2 \mathfrak{B}^2(m, \mathbf{V}, b_n)}}\right) \quad a.co.$$

Result concerns the asymptotic normality of $\widehat{DE}_\tau(\mathbf{V})$. For this asymptotic result, we state that $Z \xrightarrow{\mathcal{D}} N(\mu, \sigma^2)$ means that Z follows a normal distribution with mean μ and variance σ^2 . The symbol $\xrightarrow{\mathcal{D}}$ denotes convergence in distribution. Thus, our second main result is stated in the following theorem.

Theorem 3.2. *Under the hypotheses, consider that **DE1** and **DB1–DB3** are satisfied, and if*

$$\frac{n^2 \mathfrak{B}^2(m, \mathbf{V}, b_n)}{\mathfrak{A}(m, \mathbf{V}, b_n)} b_n^{2r} \rightarrow 0 \quad \text{as } n \rightarrow \infty,$$

then we have, for all $\mathbf{V} \in \mathcal{V}$,

$$\left(\frac{n^2 \mathfrak{B}^2(m, \mathbf{V}, b_n)}{\mathfrak{A}(m, \mathbf{V}, b_n) \sigma_\tau^2(\mathbf{V})} \right)^{\frac{1}{2}} (\widehat{DE}_\tau(\mathbf{V}) - DE_\tau(\mathbf{V})) \xrightarrow{\mathcal{D}} N(0, 1), \quad (8)$$

where

$$\sigma_\tau^2(\mathbf{V}) = \frac{B_2 \Delta_\tau(DE_\tau(\mathbf{V}))}{B_1^2 \Lambda_\tau^2(DE_\tau(\mathbf{V}))} \quad \text{and} \quad \mathcal{V} = \{\mathbf{V}; \sigma_\tau^2(\mathbf{V}) \neq 0\} \quad (9)$$

with

$$\gamma_\tau(DE_\tau(\mathbf{V}); \mathbf{V}) = \left(\frac{\tau}{1 - \tau} \right)^2 R_+(DE_\tau(\mathbf{V}); \mathbf{V}) + R_-(DE_\tau(\mathbf{V}); \mathbf{V}),$$

where

$$R_+(s; \mathbf{V}) = \mathbb{E} \left[(U - s)^2 \mathbb{1}_{(U-s)>0} \mid V = \mathbf{V} \right], \quad R_-(s; \mathbf{V}) = \mathbb{E} \left[(U - s)^2 \mathbb{1}_{(U-s)\leq 0} \mid V = \mathbf{V} \right]$$

and

$$\Lambda_\tau(DE_\tau(\mathbf{V})) = L'_1(DE_\tau(\mathbf{V}); \mathbf{V}) - \left(\frac{\tau}{1 - \tau} \right) L'_2(DE_\tau(\mathbf{V}); \mathbf{V}).$$

4. Experimental data analysis

The DCC model is commonly employed as important variant of multivariate GARCH (MGARCH) models. It is more relevant in financial risk assessment, particularly for its ability to fit time-varying correlations; a feature that aligns well with real-world market behavior. This adaptability makes the generalization of DCC within MGARCH modeling both theoretically and practically pertinent. It enhances risk detection accuracy by accounting the dynamic nature of financial volatility. Furthermore, in the context of multifunctional data analysis, Dynamic Value at Risk (DVaR) and Dynamic Expected Shortfall (DES) (see [20]) are the most widely used models in financial risk analysis. However, both risk measures have some limitations. For instance, DVaR lacks coherence, while DES fails to satisfy elicibility. Both issues are indispensable for risk assessment. In this context, dynamic-expectile regression emerges as a compelling alternative, effectively addressing the drawbacks of these traditional measures. Specifically, it is the only risk model that satisfies both coherence and elicibility. To illustrate this feature, we conduct a simulation experiment to compare its performance to

$$DVaR_\tau(\mathbf{V}) = \arg \min_{s \in \mathbb{R}} \mathbb{E} [(U - s)(\tau - \mathbb{1}_{[U < s]}) | V = \mathbf{V}] \quad \text{for } \tau \in]0, 1[,$$

and

$$DES_\tau(\mathbf{V}) = \mathbb{E} [U | U > DVaR_\tau(\mathbf{V}), V = \mathbf{V}] \quad \text{for } \tau \in]0, 1[.$$

$DVaR_\tau(\mathbf{V})$ is estimated by

$$\widehat{DVaR}_\tau(\mathbf{V}) = \arg \min \left\{ s \in \mathbb{R} : \frac{\sum_{i=1}^n \prod_{j=1}^m \mathfrak{L}(b_n^{-1} d_j(\mathbf{V}^j, V_i^j)) \mathbb{1}_{U_i \leq s}}{\sum_{i=1}^n \prod_{j=1}^m \mathfrak{L}(b_n^{-1} d_j(\mathbf{V}^j, V_i^j))} \geq \tau \right\}.$$

While $DES_\tau(\mathbf{V})$ is estimated by

$$\widehat{DES}_\tau(\mathbf{V}) = \frac{\sum_{i=1}^n \prod_{j=1}^m \mathfrak{L}(b_n^{-1} d_j(\mathbf{V}^j, V_i^j)) U_i \mathbb{1}_{(U_i > \widehat{DVaR}_\tau(\mathbf{V}))}}{\sum_{i=1}^n \prod_{j=1}^m \mathfrak{L}(b_n^{-1} d_j(\mathbf{V}^j, V_i^j))}.$$

For this aim, we generate artificial data based on the below nonparametric regression framework,

$$U_i = Fu(V_i) + \epsilon_i, \quad i = 1, \dots, n, \quad (10)$$

where $Fu(\cdot)$ is a known regression operator and (ϵ_i) is a sequence of independent random variables generated from a given distribution. The artificial multivariate functional GARCH process (V_i) is constructed using the DCC-MGARCH algorithm (7). Specifically, we set the parameters as $p = q =$

1 and $m = 2$, ensuring a well-defined stochastic structure, and use the *mfdata* function in the R-package *fda.usc* to generate the independent functional random variables. The operators α_1 and β_1 are established by

$$\beta_1(V^1, V^2) = \int_0^1 \beta^1(t, s)V^1(s)ds + \int_0^1 \beta^2(t, s)V^2(s)ds,$$

where $\beta^1(t, s) = 0.12((1-s)^2t^2)$, $\beta^2(t, s) = 0.12((1-t)^4s^4)$ and

$$\alpha_1(V^1, V^2) = \int_0^1 \alpha^1(t, s)V^1(s)ds + \int_0^1 \alpha^2(t, s)V^2(s)ds$$

with $\alpha^1(t, s) = 0.12((s-0.5)^2 + (t-0.5)^2)$, $\alpha^2(t, s) = 0.12((1-t)^2s^2)$. Such operators are introduced to include the theoretical assumptions, specifically the condition in **ED1**. Suppose the daily dynamics of a portfolio made up of two financial assets (Asset 1, Asset 2) are represented by the produced MFGARCH model. In Figures 1 and 2, we show the price trajectories of these two assets.

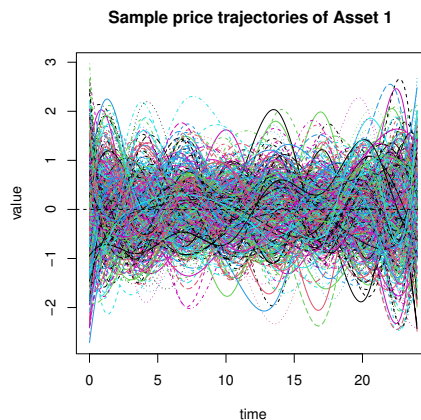


Figure 1. The first component of the MFGARCH covariate.

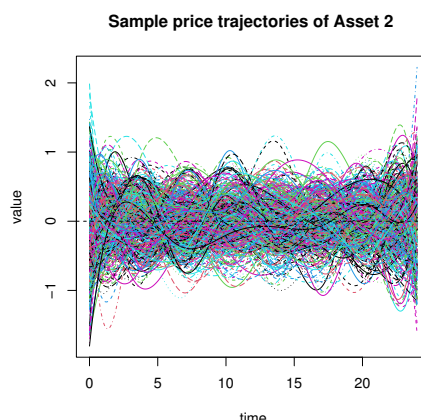


Figure 2. The second component of the MFGARCH covariate.

Concerning the output variable U_i , we assume that the function Fu is defined as the average of the daily changes of the two assets. In this simulation study, the conditional distribution of U given $V = \mathbf{V}$ is derived by shifting the distribution of the white noise term ϵ_i by the value $Fu(\mathbf{V})$. Therefore, the theoretical expectile is impacted by the distribution of ϵ . In order to cover many different tailed distributions, we conduct simulations using two types of noise distributions. The first one is the standard normal distribution ($N(0, 1)$), which represents a light-tailed case, and the second is the log-normal distribution ($\text{Log-N}(0, 1)$), known for its heavy-tailed characteristics. Recall that the principal objective of this section is to investigate the computability of the estimator $\widehat{DE}_\tau(\mathbf{V})$ using artificially generated data. It is evident that the computational feasibility of $\widehat{DE}_\tau(\mathbf{V})$ is linked to the selection of various parameters within the estimator. Therefore, for the nonparametric smoothing functional framework, the determination of the smoothing parameters and the metric's choice has a direct effect on the estimator's accuracy and reliability. Therefore, it is important to develop some selector algorithms with reasonable computational costs to choose the necessary parameters. For this aim, we use the leave-one-out cross-validation method defined by

$$b^{opt} = \arg \min_{b \in \mathbf{H}_n} \frac{1}{n} \sum_{i=1}^n \left((U_i - \widehat{DE}_\tau^{-i}(V_i))^2 |\tau - \mathbb{I}_{[U_i < \widehat{DE}_\tau^{-i}(V_i)]}| \right), \quad (11)$$

where $\widehat{DE}_\tau^{-i}(V_i)$ is the leave-one-out estimator of DE_τ . The selection rules are optimized over the set \mathbf{H}_n , which consists of positive real numbers $b(k)$ such that the ball centered at V_i with radius $b(k)$ contains exactly k nearest neighbors of V_i , where $k \in \{5, 15, 25, \dots, 0.5n\}$. In our experimental analysis, we utilize the quadratic kernel function $\mathfrak{L}(\cdot)$, defined on the interval $(0, 1)$, together with the metric induced by the spline basis functions. The parameters of \widehat{DVaR}_τ and \widehat{DES}_τ are obtained using the same rule as the routine code *funopare.quantile.lcv* in the R-package *npfda*, developed by [27]. Finally, the performance of the ED estimator is evaluated using a standard backtesting metric, allowing us to assess its empirical efficiency, formulated by

$$\text{ED}(\tau) = \frac{1}{n} \sum_{k=1}^n \left(U_i - \widehat{EST}_\tau(V_i) \right)^2 |\tau - \mathbb{I}_{[U_i < \widehat{EST}_\tau(V_i)]}|,$$

where \widehat{EST}_τ refers to one of the functions $DVaR_\tau$, DES_τ , or DE_τ . The results are summarized in Table 1, which presents the ED values for the two situations and three threshold, $\tau = 0.1, 0.05, 0.01$, with samples of $n = 50, 150, 250$.

We observe that the estimator \widehat{DE}_τ performs well under all three thresholds. However, its performance is particularly strong under the log-normal distribution, which represents a heavy-tailed case. This result is important because the effectiveness of a risk detector is mainly evaluated by its ability to handle extreme or outlier observations. Moreover, the estimator \widehat{DES}_τ shows a similar behavior, performing better than \widehat{DVaR}_τ in both light and heavy-tailed distributions. It is also worth emphasizing that, despite the complexity of the underlying model, the computation of \widehat{DE}_τ remains relatively straightforward. Moreover, the accuracy of the estimator improves as the sample size n increases.

Table 1. The ED(t) for different scenarios.

Models	Distribution	n	$\tau = 0.1$	$\tau = 0.05$	$\tau = 0.01$
\widehat{DE}_τ	$N(0, 1)$	50	0.62	0.54	0.43
		150	0.33	0.41	0.28
		250	0.25	0.18	0.13
	$Log - Normal(0, 1)$	50	0.31	0.21	0.38
		150	0.16	0.12	0.11
		250	0.06	0.07	0.03
\widehat{DVaR}_τ	$N(0, 1)$	50	0.92	0.91	0.85
		150	0.63	0.67	0.54
		250	0.42	0.47	0.41
	$Log - Normal(0, 1)$	50	1.04	1.113	.1.08
		150	0.83	0.81	0.72
		250	0.51	0.55	0.63
\widehat{DES}_τ	$N(0, 1)$	50	0.75	0.67	0.66
		150	0.51	0.58	0.46
		250	0.29	0.31	0.26
	$Log - Normal(0, 1)$	50	0.94	1.02	.99
		150	0.65	0.67	0.61
		250	0.39	0.042	0.44

5. Financial time series data analysis

The central challenge in financial risk management is to find appropriate optimal decision rules that effectively balance the trade-off between potential returns and losses of financial assets. Expectile regression, defined by its asymmetric weighting of gains and losses, offers a promising strategy for addressing this issue. Unlike traditional methods, our approach employs a non-parametric analysis of financial time series, a technique that has gained significant traction in modern big data applications. The main contribution of this study is its application of multifunctional expectile regression, a method uniquely suited for modeling the dynamic based on the time-varying relationships among multiple financial instruments. We recall that the present study differs from [19] by considering multiple functional covariates instead of a single functional covariate as in the cited work. This extension provides a more realistic and flexible framework for modeling complex relationships between several sources of risk. Typically, it allows for the simultaneous assessment of risks across different assets or market factors. Also, it permits us to explore the potential interaction that a uni-functional model fails to handle. Such a multivariate functional approach enhances both the interpretability and the predictive accuracy of the risk estimation process within a unified framework. To demonstrate its real-world applicability, we focus on three dimensional cases ($m = 3$), where $V(t)$ represents the close values for the three prominent U.S. corporations (Apple (AAPL), Amazon (AMZN), Microsoft (MSFT)) over a period from 15 January to 13 June, 2025, with a frame of 5 minutes. These time-series observations constitute a good example to analyze volatility, trends, and the interplay between macroeconomic factors and individual stock performance. The data used in this paper is available

through the link <https://stooq.com/db/h/>. The three datasets are visually presented in Figures 3–5, illustrating the high volatility as well as the different trends of the financial time series data.

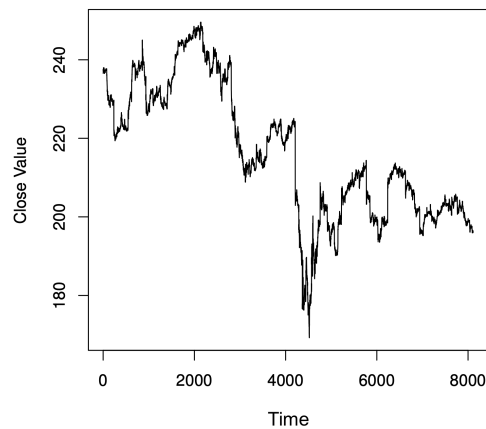


Figure 3. The close values of Apple.

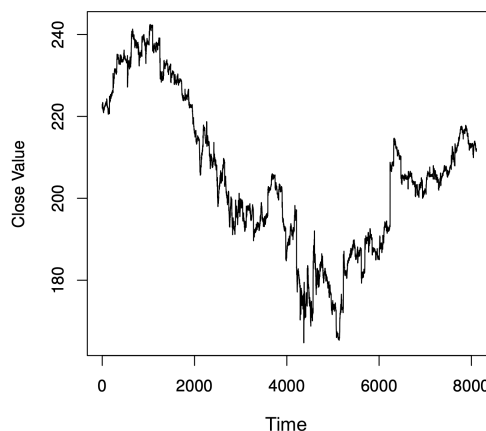


Figure 4. The close values of Amazon.

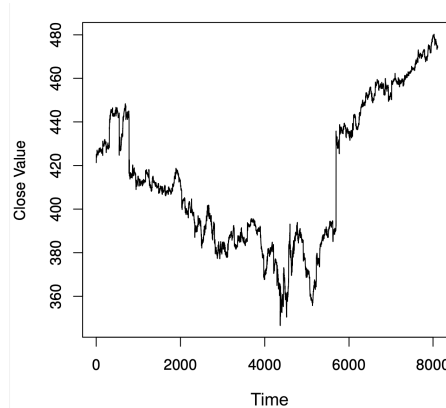


Figure 5. The close values of Microsoft.

For the practical issues, investors are often interested in log-returns, which are defined as

$$V(\cdot) = \begin{pmatrix} V^1(\cdot) \\ V^2(\cdot) \\ V^3(\cdot) \end{pmatrix} V^j(t) := 100 (\log(P(t)) - \log(P(t-1))), \quad (12)$$

where the index value at time t is represented by $P(t)$. Of course, the challenge in financial analysis is the prediction of one day before the average of the close values of the three companies. The transformed time series $V(t)$ (see Figures 3–5) exhibits the principal characteristics of financial time series data. To evaluate the performance of our approach, we compare it with traditional risk measures, particularly the dynamic value-at-risk $DVaR_\tau$ obtained by the routine code *funopare.quantile.lcv*. For a fair comparison, both methods are implemented under identical conditions, including the selection of the smoothing parameter b_n . Specifically, for the functional expectile regression, we employ a quadratic kernel defined on the interval $[0, 1]$ and adopt a PCA-based metric (we refer to [29] for more details on the definitions of these metrics). The optimal smoothing parameter b_n is determined via a local k -nearest neighbor approach. The latter is obtained by minimizing the leave-one out least square cross-validation error defined by

$$b^{optMSE} = \arg \min_{b \in \mathbf{H}_n} \frac{1}{n} \sum_{i=1}^n \left(U_i - \widehat{DE}_{0.5}^{-k}(V_i) \right)^2. \quad (13)$$

Considering some sets of \mathbf{H}_n as in previous section, we examine the impact of this parameter by comparing this rule to the selector algorithm in (11). Finally, to assess the accuracy of three estimators, we compare, in Figures 6 and 7, the estimated values (red line) against the true process for $t = 0.05$ and $t = 0.1$.

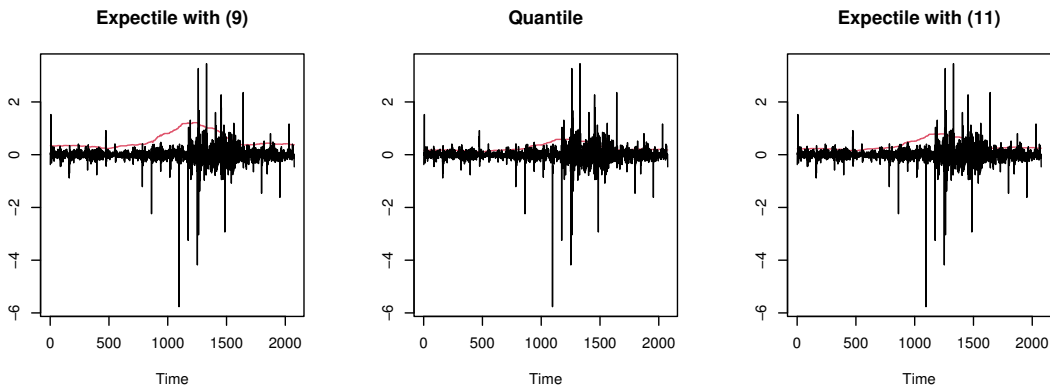


Figure 6. Comparison between the three models, $\tau = 0.05$.

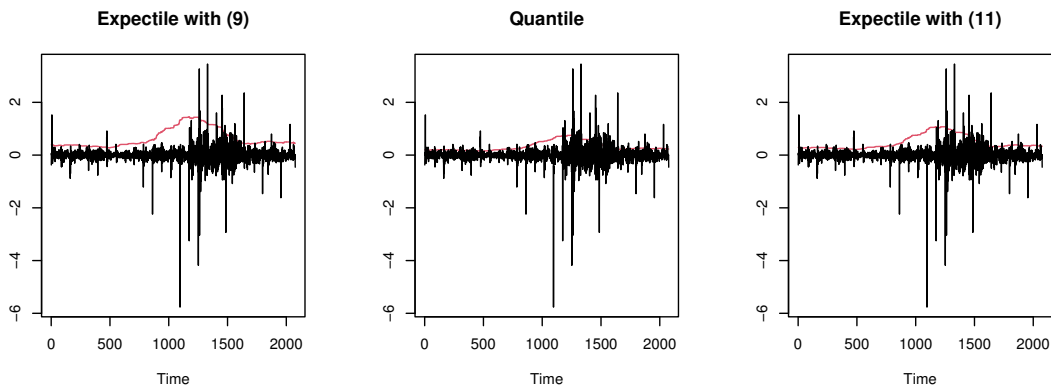


Figure 7. Comparison between the three models, $\tau = 0.15$.

The figures indicate that the dynamic expectile \widehat{DE}_t performs comparably to the \widehat{DVaR}_t function in fitting process volatility. Both models effectively identify fluctuations in volatility; however, the expectile shows superior accuracy with respect to the percentage of exceedance points. The benchmark results are presented in Table 2.

Table 2. Comparison of the exceedance percentage.

τ	0.1	0.05	0.01
\widehat{DE}_t using (11)	0.121	0.056	0.012
\widehat{DE}_t using (13)	0.162	0.075	0.0207
\widehat{DVaR}_t	0.171	0.081	0.0215

It is important to note that the estimation of the expectile function is highly sensitive to the choice of smoothing parameters. The obtained result proves that the rule proposed in (11) performs more effectively, as its exceedance percentage remains notably closer to the target threshold τ . For instance, when $\tau = 0.1$, the observed exceedance percentage is 0.12 using (11), compared to 0.16 using (13). Similarly, for $\tau = 0.05$, the exceedance rate under (11) is 0.056, whereas (13) yields 0.07. These results consistently indicate the superior precision of (11) in maintaining proximity to the desired threshold.

6. Conclusions

Real-time risk management has become a must for both investors and financial organizations due to the quick digitalization of financial transactions. This work is mainly motivated by the necessity to forecast the instantaneous risk in rapid financial dynamics. To address this challenge, we introduce a novel statistical algorithm that combines the expectile function with a multi-GARCH framework using high-frequency data. Recognizing the limitations of traditional parametric methods that often depend on restrictive linearity assumptions, we propose a more flexible nonparametric method. The theoretical part of this contribution focuses on the Borel convergence rate of the constructed estimator. The result is derived under standard conditions, allowing us to define the appropriate situation to obtain a fast estimator. However, the empirical analysis demonstrates the computational

feasibility of this approach and shows its superiority over conventional kernel-based dynamic VaR methods. Moreover, the practical implementation of our estimation requires careful consideration of several fundamental parameters, particularly the bandwidth b_n and the metric d_i . The current lack of automatic selection methods for these parameters presents a significant limitation, reducing the approach's flexibility. Consequently, developing an efficient and automated parameter selection method emerges as a crucial direction for future research. This work also opens several promising avenues for further investigation. These include extending the methodology to more complex data structures (such as spatial data or incomplete datasets) and developing alternative risk measures (like expected shortfall, or local linear estimation expectile) within the multi-GARCH framework. Such extensions would further enhance the practical applicability of real-time risk assessment in modern financial markets.

Author contributions

The authors contributed approximately equally to this work. Formal analysis, F.A.; Validation, Z.K.; Writing—review & editing, A.L. and I.M.A. All authors have read and agreed to the final version of the manuscript.

Use of Generative-AI tools declaration

The authors declare they have not used Artificial Intelligence (AI) tools in the creation of this article.

Data availability

The data used in this study are available through the link <https://stooq.com/db/h/> (accessed on 8 June, 2025).

Acknowledgments

The authors thank and extend their appreciation to the funders of this work. This work was supported by Princess Nourah bint Abdulrahman University Researchers Supporting Project number (PNURSP2025R358), Princess Nourah bint Abdulrahman University, Riyadh, Saudi Arabia, and the Deanship of Scientific Research and Graduate Studies at King Khalid University through the Research Groups Program under grant number RGP2 /456/46.

Conflict of interest

The authors declare no conflict of interest in this paper.

References

1. R. F. Engle, Autoregressive conditional heteroscedasticity with estimates of the variance of United Kingdom inflation, *Econometrica*, **50** (1982), 987–1007. <https://doi.org/10.2307/1912773>

2. T. Bollerslev, A conditionally heteroskedastic time series model for speculative prices and rates of return, *Rev. Econ. Stat.*, **69** (1987), 542–547. <https://doi.org/10.2307/1925546>
3. J. E. Yoon, J. M. Kim, S. Y. Hwang, Functional ARCH (fARCH) for high-frequency time series: Illustration, *Korean J. Appl. Stat.*, **30** (2017), 983–991.
4. C. Cerovecki, C. Francq, S. Hörmann, J. M. Zakořan, Functional GARCH models: The quasi-likelihood approach and its applications, *J. Econometrics*, **209** (2019), 353–375. <https://doi.org/10.1016/j.jeconom.2019.01.006>
5. H. Sun, B. Yu, Volatility asymmetry in functional threshold GARCH model, *J. Time Ser. Anal.*, **41** (2020), 95–109. <https://doi.org/10.1111/jtsa.12495>
6. Z. Li, H. Sun, J. Liu, A functional GARCH model with multiple constant parameters, *Comput. Econ.*, **66** (2025), 3957–3981. <https://doi.org/10.1007/s10614-025-10843-1>
7. S. Küchnert, Functional ARCH and GARCH models: A Yule–Walker approach, *Electron. J. Statist.*, **14** (2020), 4321–4360. <https://doi.org/10.1214/20-EJS1778>
8. N. Laib, D. Louani, Rates of strong consistencies of the regression function estimator for functional stationary ergodic data, *J. Stat. Plan. Infer.*, **141** (2011), 359–372. <https://doi.org/10.1016/j.jspi.2010.06.009>
9. C. M. Kuan, J. H. Yeh, Y. C. Hsu, Assessing value at risk with CARE, the conditional autoregressive expectile models, *J. Econometrics*, **150** (2009), 261–270. <https://doi.org/10.1016/j.jeconom.2008.12.002>
10. W. Ehm, T. Gneiting, A. Jordan, F. Krüger, Of quantiles and expectiles: Consistent scoring functions, Choquet representations and forecast rankings, *J. R. Stat. Soc. B*, **78** (2016), 505–562. <https://doi.org/10.1111/rssb.12154>
11. F. Bellini, V. Bignozzi, G. Puccetti, Conditional expectiles, time consistency and mixture convexity properties, *Insur. Math. Econ.*, **82** (2018), 117–123. <http://doi.org/10.2139/ssrn.3009354>
12. R. Koenker, G. Bassett Jr., Regression quantiles, *Econometrica*, **46** (1978), 33–50.
13. R. Koenker, G. Bassett Jr., Robust tests for heteroscedasticity based on regression quantiles, *Econometrica*, **50** (1982), 43–61.
14. A. Daouia, S. Girard, G. Stupler, Estimation of tail risk based on extreme expectiles, *J. R. Stat. Soc. B*, **80** (2018), 263–292. <https://doi.org/10.1111/rssb.12254>
15. B. Efron, Regression percentiles using asymmetric squared error loss, *Stat. Sin.*, **1** (1991), 93–125.
16. H. Holzmann, B. Klar, Expectile asymptotics, *Electron. J. Statist.*, **10** (2016), 2355–2371. <https://doi.org/10.1214/16-EJS1173>
17. V. Maume-Deschamps, D. Rullière, K. Said, Multivariate extensions of expectiles risk measures, *Depend. Model.*, **5** (2017), 20–44. <https://doi.org/10.1515/demo-2017-0002>
18. V. Krätschmer, H. Zähle, Statistical inference for expectile-based risk measures, *Scand. J. Stat.*, **44** (2017), 425–454. <https://doi.org/10.1111/sjos.12259>
19. M. Mohammedi, S. Bouzebda, A. Laksaci, The consistency and asymptotic normality of the kernel type expectile regression estimator for functional data, *J. Multivariate Anal.*, **181** (2021), 104673. <https://doi.org/10.1016/j.jmva.2020.104673>

20. I. M. Almanjahie, S. Bouzebda, Z. Kaid, A. Laksaci, Nonparametric estimation of expectile regression in functional dependent data, *J. Nonparametr. Stat.*, **34** (2022), 250–281. <https://doi.org/10.1080/10485252.2022.2027412>

21. F. Alshahrani, I. M. Almanjahie, Z. C. Elmezouar, Z. Kaid, A. Laksaci, M. Rachdi, Functional ergodic time series analysis using expectile regression, *Mathematics*, **10** (2022), 3919. <https://doi.org/10.3390/math10203919>

22. M. Lux, W. K. Härdle, S. Lessmann, Data driven value-at-risk forecasting using a SVR-GARCH-KDE hybrid, *Comput. Stat.*, **35** (2020), 947–981. <https://doi.org/10.1007/s00180-019-00934-7>

23. T. H. Kim, H. White, On more robust estimation of skewness and kurtosis, *Financ. Res. Lett.*, **1** (2004), 56–73. [https://doi.org/10.1016/S1544-6123\(03\)00003-5](https://doi.org/10.1016/S1544-6123(03)00003-5)

24. H. Cardot, C. Crambes, P. Sarda, Quantile regression when the covariates are functions, *J. Nonparametr. Stat.*, **17** (2005), 841–856. <https://doi.org/10.1080/10485250500303015>

25. R. Engle, Dynamic conditional correlation: A simple class of multivariate generalized autoregressive conditional heteroskedasticity models, *J. Bus. Econ. Stat.*, **20** (2002), 339–350. <https://doi.org/10.1198/073500102288618487>

26. C. Francq, J. M. Zakoian, *GARCH models: structure, statistical inference and financial applications*, Wiley, 2019.

27. F. Ferraty, P. Vieu, *Nonparametric functional data analysis: Theory and practice*, New York: Springer, 2006. <https://doi.org/10.1007/0-387-36620-2>

28. V. I. Bogachev, *Gaussian measures*, American Mathematical Society, 1998.

29. K. Benhenni, F. Ferraty, M. Rachdi, P. Vieu, Local smoothing regression with functional data, *Comput. Stat.*, **22** (2007), 353–369. <https://doi.org/10.1007/s00180-007-0045-0>

30. P. Gaenssler, E. Haeusler, On martingale central limit theory, In: Dependence in probability and statistics, Boston: Birkhäuser, 1986, 303–334. https://doi.org/10.1007/978-1-4615-8162-8_13

Appendix

Proof of Theorem 3.1

We start with

$$v_n = \epsilon_0 \left(b_n^{\min(k_1, k_2)} + \sqrt{\frac{\mathfrak{A}(m, \mathbf{V}, b_n) \log n}{n^2 \mathfrak{B}^2(m, \mathbf{V}, b_n)}} \right) \quad \text{for some constant } \epsilon_0 > 0. \quad (14)$$

So, our aim is to establish the probability bound, i.e.,

$$\sum_{n=1}^{\infty} \mathbb{P}(|\widehat{DE}_{\tau}(\mathbf{V}) - DE_{\tau}(\mathbf{V})| > v_n) \leq \sum_{n=1}^{\infty} \mathbb{P}\left(\sup_{s \in \mathcal{I}_a} |\widehat{L}(s; \mathbf{V}) - L(s; \mathbf{V})| \geq Cv_n\right) < \infty, \quad (15)$$

where $\mathcal{I}_a = [DE_{\tau}(\mathbf{V}) - a, DE_{\tau}(\mathbf{V}) + a]$. This inequality immediately yields our main result through the following uniform approximation,

$$\sup_{s \in \mathcal{I}_a} |\widehat{L}(s; \mathbf{V}) - L(s; \mathbf{V})| = O_{a.co.}(v_n). \quad (16)$$

The claimed results are based on the following decomposition,

$$\widehat{L}(s; \mathbf{V}) - L(s; \mathbf{V}) = \underbrace{\widehat{\Upsilon}_{1n}(s; \mathbf{V})}_{\text{Bias term}} + \underbrace{\frac{\widehat{\Upsilon}_{2n}(s; \mathbf{V})}{\widehat{L}_D(s; \mathbf{V})} + \frac{\widehat{\Upsilon}_{3n}(s; \mathbf{V})}{\widehat{L}_D(s; \mathbf{V})}}_{\text{Stochastic terms}}. \quad (17)$$

The constituent components are defined as

$$\begin{aligned} \widehat{\Upsilon}_{3n}(s; \mathbf{V}) &:= \left(\widehat{L}_N(s; \mathbf{V}) - \overline{L}_N(s; \mathbf{V}) \right) - L(s; \mathbf{V}) \left(\widehat{L}_D(s; \mathbf{V}) - \overline{L}_D(s; \mathbf{V}) \right) \\ \widehat{\Upsilon}_{1n}(s; \mathbf{V}) &:= \frac{\overline{L}_N(s; \mathbf{V})}{\widehat{L}_D(s; \mathbf{V})} - L(s; \mathbf{V}) \\ \widehat{\Upsilon}_{2n}(s; \mathbf{V}) &:= -\widehat{\Upsilon}_{1n} \left(\widehat{L}_D(s; \mathbf{V}) - \overline{L}_D(s; \mathbf{V}) \right), \end{aligned}$$

with

$$\begin{aligned} \widehat{L}_N(s; \mathbf{V}) &= \frac{1}{n\mathfrak{B}(m, \mathbf{V}, b)} \sum_{i=1}^n \prod_{j=1}^m \mathfrak{L}(b_n^{-1} d_j(\mathbf{V}^j, V_i^j)) (U_i - t)_- \\ \overline{L}_N(s; \mathbf{V}) &= \frac{1}{n\mathfrak{B}(m, \mathbf{V}, b)} \sum_{i=1}^n \mathbb{E} \left[\prod_{j=1}^m \mathfrak{L}(b_n^{-1} d_j(\mathbf{V}^j, V_i^j)) (U_i - t)_- \middle| \mathfrak{G}_{i-1} \right] \\ \widehat{L}_D(s; \mathbf{V}) &= \frac{1}{n\mathfrak{B}(m, \mathbf{V}, b)} \sum_{i=1}^n \prod_{j=1}^m \mathfrak{L}(b_n^{-1} d_j(\mathbf{V}^j, V_i^j)) (U_i - s)_+ \\ \overline{L}_D(s; \mathbf{V}) &= \frac{1}{n\mathfrak{B}(m, \mathbf{V}, b)} \sum_{i=1}^n \mathbb{E} \left[\prod_{j=1}^m \mathfrak{L}(b_n^{-1} d_j(\mathbf{V}^j, V_i^j)) (U_i - s)_+ \middle| \mathfrak{G}_{i-1} \right], \end{aligned}$$

where $(U)_\pm = U \mathbb{1}_{\{U \gtrless 0\}}$ denotes the positive/negative part.

Finally, we establish Theorem 3.1 through a series of technical lemmas, presented below.

Lemma A.1. *Considering postulates **DE2**, **DE4**, and **DE5**, we obtain*

$$\sup_{s \in [DE_\tau(\mathbf{V}) - a, DE_\tau(\mathbf{V}) + a]} \left| \widehat{L}_D(s; \mathbf{V}) - \overline{L}_D(s; \mathbf{V}) \right| = O_{a.co.} \left(\sqrt{\frac{\mathfrak{A}(m, \mathbf{V}, b_n) \log n}{n^2 \mathfrak{B}^2(m, \mathbf{V}, b_n)}} \right)$$

and

$$\sup_{s \in [DE_\tau(\mathbf{V}) - a, DE_\tau(\mathbf{V}) + a]} \left| \widehat{L}_N(s; \mathbf{V}) - \overline{L}_N(s; \mathbf{V}) \right| = O_{a.co.} \left(\sqrt{\frac{\mathfrak{A}(m, \mathbf{V}, b_n) \log n}{n^2 \mathfrak{B}^2(m, \mathbf{V}, b_n)}} \right).$$

Proof of Lemma A.1

The proofs of both assertions are analogous. For brevity, we establish the second assertion and subsequently deduce the first. The compactness of $[DE_\tau(\mathbf{V}) - a, DE_\tau(\mathbf{V}) + a]$ permits us to write

$$[DE_\tau(\mathbf{V}) - a, DE_\tau(\mathbf{V}) + a] \subset \bigcup_{j=1}^{d_n} (\nu_j - l_n, \nu_j + l_n)$$

with $l_n = n^{-1/2}$ and $d_n = O(n^{1/2})$. The monotony of $\widehat{L}_N(\cdot; \mathbf{V})$ and $\overline{L}_N(\cdot; \mathbf{V})$ gives, $\forall 1 \leq j \leq d_n$,

$$\widehat{L}_N((\nu_j - l_n); \mathbf{V}) \leq \sup_{s \in (\nu_j - l_n, \nu_j + l_n)} \widehat{L}_N(s; \mathbf{V}) \leq \widehat{L}_N((\nu_j + l_n); \mathbf{V})$$

and

$$\overline{L}_N((\nu_j - l_n); \mathbf{V}) \leq \sup_{s \in (\nu_j - l_n, \nu_j + l_n)} \overline{L}_N(s; \mathbf{V}) \leq \overline{L}_N((\nu_j + l_n); \mathbf{V}).$$

Clearly,

$$\begin{aligned} & \sup_{s \in [DE_\tau(\mathbf{V}) - a, DE_\tau(\mathbf{V}) + a]} |\widehat{L}_N(s; \mathbf{V}) - \overline{L}_N(s; \mathbf{V})| \\ & \leq \max_{1 \leq j \leq d_n} \max_{z \in \{\nu_j - l_n, \nu_j + l_n\}} |\widehat{L}_N(z; \mathbf{V}) - \overline{L}_N(z; \mathbf{V})| + 2Cl_n \quad \text{almost completely.} \end{aligned}$$

Observe that, under **DE4**, we have

$$l_n = o\left(\sqrt{\frac{\mathfrak{A}(m, \mathbf{V}, b_n) \log n}{n^2 \mathfrak{B}^2(m, \mathbf{V}, b_n)}}\right).$$

The remaining step in proving this lemma requires showing that

$$\max_{1 \leq j \leq d_n} \max_{z \in \{\nu_j - l_n, \nu_j + l_n\}} |\widehat{L}_N(z; \mathbf{V}) - \overline{L}_N(z; \mathbf{V})| = O_{a.co.}\left(\sqrt{\frac{\mathfrak{A}(m, \mathbf{V}, b_n) \log n}{n^2 \mathfrak{B}^2(m, \mathbf{V}, b_n)}}\right).$$

To accomplish this, it is sufficient to consider the fact that

$$\forall \varepsilon > 0 \quad \mathbb{P}\left(\max_{z \in \mathcal{G}_n} |\widehat{L}_N(z; \mathbf{V}) - \overline{L}_N(z; \mathbf{V})| > \varepsilon\right) \leq \sum_{z \in \mathcal{G}_n} \mathbb{P}\left(|\widehat{L}_N(z; \mathbf{V}) - \overline{L}_N(z; \mathbf{V})| > \varepsilon\right),$$

where $\mathcal{G}_n = \{\nu_j - l_n, \nu_j + l_n, 1 \leq j \leq d_n\}$. Since the response variable U may be unbounded, we employ a truncation method to facilitate the analysis. Specifically, we define modified versions of the estimators:

$$\widehat{L}_N^*(z; \mathbf{V}) = \frac{1}{n \mathfrak{B}(m, \mathbf{V}, b)} \sum_{i=1}^n \mathfrak{L}_i U_i^{-*},$$

$$\overline{L}_N^*(z; \mathbf{V}) = \frac{1}{n \mathfrak{B}(m, \mathbf{V}, b)} \sum_{i=1}^n \mathbb{E}[\mathfrak{L}_i U_i^{-*} | \mathfrak{G}_{i-1}],$$

where

$$U_i^{-*} = U_i^- \mathbb{1}_{\{|U^-| < \gamma_n\}},$$

with $\gamma_n = n^{\delta/q}$ and $\mathfrak{L}_i = \prod_{j=1}^m \mathfrak{L}(b_n^{-1} d_j(\mathbf{V}^j, V_i^j))$. This assertion can be verified through the following three propositions:

$$d_n \max_{z \in \mathcal{L}_n} |\overline{L}_N^*(z; \mathbf{V}) - \overline{L}_N(z; \mathbf{V})| = O_{a.co.}\left(\sqrt{\frac{\mathfrak{A}(m, \mathbf{V}, b_n) \log n}{n^2 \mathfrak{B}^2(m, \mathbf{V}, b_n)}}\right), \quad (18)$$

$$d_n \max_{z \in \mathcal{L}_n} \left| \widehat{L}_N(z; \mathbf{V}) - \widehat{L}_N^*(z; \mathbf{V}) \right| = O_{a.co.} \left(\sqrt{\frac{\mathfrak{A}(m, \mathbf{V}, b_n) \log n}{n^2 \mathfrak{B}^2(m, \mathbf{V}, b_n)}} \right), \quad (19)$$

and

$$d_n \max_{z \in \mathcal{L}_n} \left| \widehat{L}_N^*(z; \mathbf{V})(x, z) - \overline{L}_N^*(z; \mathbf{V}) \right| = O_{a.co.} \left(\sqrt{\frac{\mathfrak{A}(m, \mathbf{V}, b_n) \log n}{n^2 \mathfrak{B}^2(m, \mathbf{V}, b_n)}} \right). \quad (20)$$

Let us consider statement (18). We have, for all $z \in \mathcal{G}_n$, that

$$\left| \overline{L}_N^*(z; \mathbf{V}) - \overline{L}_N(z; \mathbf{V}) \right| \leq C \frac{1}{n \mathfrak{B}(m, \mathbf{V}, b)} \sum_{i=1}^n \mathbb{E} \left[\left| U_i^- \right| \mathbb{1}_{\{|U_i^-| \geq \gamma_n\}} \mathfrak{L}_i \mid \mid \mathfrak{G}_{i-1} \right].$$

Apply Hölder inequality, for $\alpha_1 = \frac{q}{2}$ with β_1 , to obtain

$$\frac{1}{\alpha_1} + \frac{1}{\beta_1} = 1.$$

Use **DE2** and **DE5** to show that, for all $z \in \mathcal{L}_n$,

$$\begin{aligned} \mathbb{E} \left[\left| U_i^- \right| \mathbb{1}_{\{|U_i^-| \geq \gamma_n\}} \mathfrak{L}_i \mid \mid \mathfrak{G}_{i-1} \right] &\leq \mathbb{E}^{1/\alpha_1} \left[\left| U_i^{\alpha_1} \right| \mathbb{1}_{\{|U_i^-| \geq \gamma_n\}} \mid \mid \mathfrak{G}_{i-1} \right] \mathbb{E}^{1/\beta_1} \left[\mathfrak{L}_i^{\beta_1} \mid \mid \mathfrak{G}_{i-1} \right] \\ &\leq \gamma_n^{-1} \mathbb{E}^{1/\alpha_1} \left[\left| U_i^{2\alpha_1} \right| \mid \mid \mathfrak{G}_{i-1} \right] \mathbb{E}^{1/\beta_1} \left[\mathfrak{L}_i^{\beta_1} \mid \mid \mathfrak{G}_{i-1} \right] \\ &\leq \gamma_n^{-1} \mathbb{E}^{1/\alpha_1} [|U^q| \mid \mid \mathfrak{G}_{i-1}] \mathbb{E}^{1/\beta_1} \left[\mathfrak{L}_i^{\beta_1} \mid \mid \mathfrak{G}_{i-1} \right] \\ &\leq C \gamma_n^{-1} \mathfrak{B}_i^{1/\beta_1}(m, \mathbf{V}, b_n). \end{aligned}$$

We obtain

$$d_n \max_{z \in \mathcal{L}_n} \left| \overline{L}_N^*(z; \mathbf{V}) - \overline{L}_N(z; \mathbf{V}) \right| \leq C n^{1/2-\delta/q} \frac{1}{n \mathfrak{B}(m, \mathbf{V}, b)} \sum_{i=1}^n \mathfrak{B}_i^{1/\beta_1}(m, \mathbf{V}, b_n).$$

Using the fact that $\delta > q/2$, we get statement (18). Next, Markov's inequality is used to prove (19), where, $\forall z \in \mathcal{L}_n, \forall \epsilon > 0$,

$$\begin{aligned} \mathbb{P} \left(\left| \widehat{L}_N(z; \mathbf{V}) - \widehat{L}_N^*(z; \mathbf{V}) \right| > \epsilon \right) &\leq \sum_{i=1}^n \mathbb{P} \left(|U_i^-| > n^{\delta/q} \right) \\ &\leq n \mathbb{P} \left(|U_i^-| > n^{\delta/q} \right) \\ &\leq n^{1-\delta} \mathbb{E} [U^q]. \end{aligned}$$

Thus, for $\delta > 3$, there exist $\xi > 0$ such that

$$d_n \max_{z \in \mathcal{L}_n} \mathbb{P} \left(\left| \widehat{L}_N^*(z; \mathbf{V})(x, z) - \overline{L}_N^*(z; \mathbf{V}) \right| > \epsilon_0 \left(\sqrt{\frac{\mathfrak{A}(m, \mathbf{V}, b_n) \log n}{n^2 \mathfrak{B}^2(m, \mathbf{V}, b_n)}} \right) \right) \leq n^{3/2-\delta} < C n^{-1-\xi}.$$

We now prove (20). To this end, we define, for all $z \in \mathcal{G}_n$,

$$\Gamma_i(z; \mathbf{V}) = (\mathfrak{L}_i U_i^{-*} - \mathbb{E} [\mathfrak{L}_i U_i^{-*} \mid \mid \mathfrak{G}_{i-1}]).$$

The remainder of the proof utilizes exponential tail bounds for martingale difference sequences,

$$|\Gamma_i(z; \mathbf{V})| \leq \frac{C\gamma_n}{n\mathfrak{B}(m, \mathbf{V}, b)}.$$

So, all that remains is to evaluate, asymptotically, the conditional variance of $\Gamma_i(z; \mathbf{V})$, i.e.,

$$\begin{aligned} & \mathbb{E} \left[|\mathfrak{L}_i U_i^-|^2 \mid \mathfrak{G}_{i-1} \right] \\ &= \mathbb{E} \left[\mathbb{E} \left[|\mathfrak{L}_i|^2 | U_i^-|^2 \mid V \right] \mid \mathfrak{G}_{i-1} \right] \\ &= \mathbb{E} \left[\mathbb{E} \left[|U_i^-|^2 \mid V \right] \mathfrak{L}_i^2 \mid \mathfrak{G}_{i-1} \right] \\ &= C \mathbb{E} \left[\mathfrak{L}_i^2 \mid \mathfrak{G}_{i-1} \right]. \end{aligned}$$

Obviously,

$$\mathbb{E} \left[|\mathfrak{L}_i U_i^-|^2 \mid \mathfrak{G}_{i-1} \right] \leq C\mathfrak{B}_i(m, \mathbf{V}, b).$$

Hence, we obtain

$$\sum_{i=1}^n \mathbb{E} \left[\Gamma_i^2(z; \mathbf{V}) \right] = O(\mathfrak{A}(m, \mathbf{V}, b_n)). \quad (21)$$

Therefore, we get, for all $\eta > 0$ and for all $z \in \mathcal{G}_n$, that

$$\begin{aligned} & \mathbb{P} \left(\left| \widehat{L}_N(z; \mathbf{V}) - \bar{L}_N(z; \mathbf{V}) \right| > \eta \sqrt{\frac{\mathfrak{A}(m, \mathbf{V}, b_n) \log n}{n^2 \mathfrak{B}^2(m, \mathbf{V}, b_n)}} \right) \\ & \leq 2 \exp \left\{ -\eta^2 \frac{\mathfrak{A}(m, \mathbf{V}, b_n) \log n}{2 \left((\mathfrak{A}(m, \mathbf{V}, b_n)) + C \left(\eta \sqrt{\mathfrak{A}(m, \mathbf{V}, b_n) \log n} \right) \right)} \right\} \\ & \leq 2 \exp \left\{ -\frac{\eta^2 \log n}{2 \left(\left(1 + C\eta \left(\sqrt{\frac{\log n}{\mathfrak{A}(m, \mathbf{V}, b_n)}} \right) \right) \right)} \right\}. \end{aligned}$$

Then, as $d_n \leq Cl_n^{-1}$, we have

$$\begin{aligned} & \sum_{z \in \mathcal{G}_n} \mathbb{P} \left(\left| \widehat{L}_N(z; \mathbf{V}) - \bar{L}_N(z; \mathbf{V}) \right| > \eta \sqrt{\frac{\mathfrak{A}(m, \mathbf{V}, b_n) \log n}{n^2 \mathfrak{B}^2(m, \mathbf{V}, b_n)}} \right) \\ & \leq 2d_n \max_{z \in \mathcal{G}_n} \mathbb{P} \left(\left| \widehat{L}_N(z; \mathbf{V}) - \bar{L}_N(z; \mathbf{V}) \right| > \eta \sqrt{\frac{\mathfrak{A}(m, \mathbf{V}, b_n) \log n}{n^2 \mathfrak{B}^2(m, \mathbf{V}, b_n)}} \right) \\ & \leq C'n^{-C\eta^2+1/2}. \end{aligned}$$

Similarly,

$$\sum_{z \in \mathcal{G}_n} \mathbb{P} \left(\left| \widehat{L}_D(z; \mathbf{V}) - \bar{L}_D(z; \mathbf{V}) \right| > \eta \sqrt{\frac{\mathfrak{A}(m, \mathbf{V}, b_n) \log n}{n^2 \mathfrak{B}^2(m, \mathbf{V}, b_n)}} \right)$$

$$\begin{aligned} &\leq 2d_n \max_{z \in \mathcal{G}_n} \mathbb{P} \left(\left| \widehat{L}_D(z; \mathbf{V}) - \bar{L}_D(z; \mathbf{V}) \right| > \eta \sqrt{\frac{\mathfrak{A}(m, \mathbf{V}, b_n) \log n}{n^2 \mathfrak{B}^2(m, \mathbf{V}, b_n)}} \right) \\ &\leq C' n^{-C\eta^2+1/2}. \end{aligned}$$

Thus, selecting an appropriate value of η completes the proof and deduces that

$$\sup_{s \in [DE_\tau(\mathbf{V})-a, DE_\tau(\mathbf{V})+a]} \left| \widehat{L}_D(s; \mathbf{V}) - \bar{L}_D(s; \mathbf{V}) \right| = O_{a.co.} \left(\sqrt{\frac{\mathfrak{A}(m, \mathbf{V}, b_n) \log n}{n^2 \mathfrak{B}^2(m, \mathbf{V}, b_n)}} \right)$$

and

$$\sup_{s \in [DE_\tau(\mathbf{V})-a, DE_\tau(\mathbf{V})+a]} \left| \widehat{L}_N(s; \mathbf{V}) - \bar{L}_N(s; \mathbf{V}) \right| = O_{a.co.} \left(\sqrt{\frac{\mathfrak{A}(m, \mathbf{V}, b_n) \log n}{n^2 \mathfrak{B}^2(m, \mathbf{V}, b_n)}} \right).$$

□

Lemma A.2. *Using postulates of Lemma A.1, we get*

$$\exists C > 0 \quad \sum_{n=1}^{\infty} \mathbb{P} \left(\sup_{s \in [DE_\tau(\mathbf{V})-a, DE_\tau(\mathbf{V})+a]} \left| \widehat{L}_D(s; \mathbf{V}) \right| \leq C \right) < \infty.$$

Proof of Lemma A.2

By the previous lemma, it follows that for every s in $[DE_\tau(\mathbf{V}) - a, DE_\tau(\mathbf{V}) + a]$ there exists a constant $C_s > 0$ such that

$$\sup_{s \in [DE_\tau(\mathbf{V})-a, DE_\tau(\mathbf{V})+a]} \left| \bar{L}_D(s; \mathbf{V}) - C_s \right| = o_{a.co.}(1). \quad (22)$$

This reveals that

$$\begin{aligned} &\inf_{s \in [DE_\tau(\mathbf{V})-a, DE_\tau(\mathbf{V})+a]} \bar{L}_D(s; \mathbf{V}) \leq \frac{C_{s_0}}{2} \\ \Rightarrow \exists s_0 \in [DE_\tau(\mathbf{V})-a, DE_\tau(\mathbf{V})+a], \quad &\text{such that} \quad C_{s_0} - \bar{L}_D(s_0; \mathbf{V}) > \frac{C_{s_0}}{2} \\ \Rightarrow \sup_{s \in [DE_\tau(\mathbf{V})-a, DE_\tau(\mathbf{V})+a]} |C_s - \bar{L}_D(s; \mathbf{V})| &> \frac{C_{s_0}}{2}. \end{aligned}$$

We deduce that

$$\mathbb{P} \left(\inf_{s \in [DE_\tau(\mathbf{V})-a, DE_\tau(\mathbf{V})+a]} \bar{L}_D(s; \mathbf{V}) \leq \frac{C_{s_0}}{2} \right) \leq \mathbb{P} \left(\sup_{s \in [DE_\tau(\mathbf{V})-a, DE_\tau(\mathbf{V})+a]} |C_s - \bar{L}_D(s; \mathbf{V})| > \frac{C_{s_0}}{2} \right).$$

Consequently,

$$\sum_{i=1}^{\infty} \left(\inf_{s \in [DE_\tau(\mathbf{V})-a, DE_\tau(\mathbf{V})+a]} \bar{L}_D(s; \mathbf{V}) \leq \frac{C_{s_0}}{2} \right) < \infty.$$

□

Lemma A.3. *Considering postulates **DE2–DE6**, we obtain*

$$\sup_{s \in [DE_\tau(\mathbf{V})-a, DE_\tau(\mathbf{V})+a]} |\widehat{\Upsilon}_{1n}(s; \mathbf{V})| = O_{a.co.} \left(b_n^{\min(k_1, k_2)} \right).$$

Proof of Lemma A.3

Using

$$\widehat{\Upsilon}_{1n}(s; \mathbf{V}) \leq \frac{1}{L_D(s; \mathbf{V})n\mathfrak{B}(m, \mathbf{V}, b_n)} \sum_{i=1}^n \mathbb{E} [\mathfrak{L}_i | L_1(t; \mathbf{V}_i) - L_2(t; \mathbf{V}_i)L(s; \mathbf{V})| \mathfrak{G}_{i-1}],$$

it is clear that

$$|L_1(s; \mathbf{V}_i) - L_2(s; \mathbf{V}_i)L(s; \mathbf{V})| \leq |L_1(s; \mathbf{V}_i) - L_1(s; \mathbf{V})| + |L(s; \mathbf{V})| |L_2(t; \mathbf{V}_i) - L_2(s; \mathbf{V})|.$$

By **DE3**, we obtain, for all $s \in [DE_\tau(\mathbf{V}) - a, DE_\tau(\mathbf{V}) + a]$, that

$$\mathbb{I}_{\{B(x, b_n)\}}(X_i) |L_1(t; \mathbf{V}_i) - L_1(s; \mathbf{V})| \leq Cb_n^{k_1}$$

and

$$\mathbb{I}_{\{B(x, b_n)\}}(X_i) |L_2(t; \mathbf{V}_i) - L_2(s; \mathbf{V})| \leq Cb_n^{k_2}.$$

By integrating these bounds with the result from Lemma A.2, we obtain

$$\sup_{s \in [DE_\tau(\mathbf{V}) - a, DE_\tau(\mathbf{V}) + a]} |\widehat{\Upsilon}_{1n}(s; \mathbf{V})| = O_{a.co.}(b_n^{\min(k_1, k_2)}).$$

□

Proof of Theorem 3.2

For the sake of shortness, the proof of this result is given briefly because it is based on standard arguments. Let us now introduce

$$Z_n = \left(\frac{n^2 \mathfrak{B}^2(m, \mathbf{V}, b_n)}{\mathfrak{A}(m, \mathbf{V}, b_n) \sigma_\tau^2(\mathbf{V})} \right)^{\frac{1}{2}} (\widehat{DE}_\tau(\mathbf{V}) - DE_\tau(\mathbf{V})).$$

For $z \in \mathbb{R}$, we set

$$\delta_\tau(z) = DE_\tau(\mathbf{V}) + z(n\phi_x(h))^{-\frac{1}{2}} \sigma_\tau.$$

We have the following decomposition.

$$\begin{aligned} \mathbb{P}(Z_n \leq z) &= \mathbb{P}(\widehat{DE}_\tau(\mathbf{V}) \leq \delta_\tau(z)) = \mathbb{P}(\{\widehat{DE}_\tau(\mathbf{V}) \leq \delta_\tau(z)\} \cap \{\widehat{L}_D(\delta_\tau(z); \mathbf{V}) = 0\}) \\ &\quad + \mathbb{P}(\{\widehat{DE}_\tau(\mathbf{V}) \leq \delta_\tau(z)\} \cap \{\widehat{L}_D(\delta_\tau(z); \mathbf{V}) \neq 0\}) \end{aligned} \quad (23)$$

Therefore, our main result is a consequence of

$$\begin{aligned} &\left(\frac{n^2 \mathfrak{B}^2(m, \mathbf{V}, b_n)}{\mathfrak{A}(m, \mathbf{V}, b_n) \sigma_\tau^2(\mathbf{V})} \right)^{\frac{1}{2}} (\Lambda_\tau(DE_\tau(\mathbf{V}))^{-1} (\widehat{L}_N(\delta_\tau(z); \mathbf{V}) - \overline{L}_N(\delta_\tau(z); \mathbf{V})) \\ &\quad - \frac{\tau}{1-\tau} (\widehat{L}_D(\delta_\tau(z); \mathbf{V}) - \overline{L}_D(\delta_\tau(z); \mathbf{V}))) \xrightarrow{\mathcal{D}} \mathcal{N}(0, 1) \end{aligned} \quad (24)$$

and

$$\left(\frac{n^2 \mathfrak{B}^2(m, \mathbf{V}, b_n)}{\mathfrak{A}(m, \mathbf{V}, b_n) \sigma_\tau^2(\mathbf{V})} \right)^{\frac{1}{2}} (\Lambda_\tau (\overline{L}_N(\delta_\tau(z); \mathbf{V}) - \frac{\tau}{1-\tau} \overline{L}_D(\delta_\tau(z); \mathbf{V}))$$

$$- \mathbb{E} \left[\widehat{L}_N(\delta_\tau(z); \mathbf{V}) \right] - \frac{\tau}{1-\tau} \mathbb{E} \left[\widehat{L}_D(\delta_\tau(z); \mathbf{V}) \right] \right) = (\Lambda_\tau (DE_\tau(\mathbf{V})) z + o(1). \quad (25)$$

The proof of (25) is similar to the evaluation of $\widehat{\Upsilon}_{1n}(s; \mathbf{V})$ in Lemma A.3. For (24) we put, for $i = 1, \dots, n$,

$$\eta_{ni} = \frac{1}{n \mathfrak{B}(m, \mathbf{V}, b_n)} \mathfrak{L}_i(U_i - \delta_\tau(z)) \left(\frac{\tau}{1-\tau} \mathbb{1}_{\mathcal{I}_i} + \mathbb{1}_{\mathcal{I}_i^c} \right) \quad (26)$$

with $\mathcal{I}_i = \{U_i > \delta_\tau(z)\}$ and $\mathcal{I}_i^c = \{U_i \leq \delta_\tau(z)\}$. Define $\zeta_{ni} := \eta_{ni} - \mathbb{E}[\eta_{ni} | F_{i-1}]$. Under this consideration we have

$$\begin{aligned} & \left(\frac{n^2 \mathfrak{B}^2(m, \mathbf{V}, b_n)}{\mathfrak{A}(m, \mathbf{V}, b_n) \sigma_\tau^2(\mathbf{V})} \right)^{\frac{1}{2}} (\Lambda_\tau (DE_\tau(\mathbf{V})))^{-1} \left((\widehat{L}_N(\delta_\tau(z); \mathbf{V}) - \overline{L}_N(\delta_\tau(z); \mathbf{V})) \right. \\ & \quad \left. - \frac{\tau}{1-\tau} (\widehat{L}_D(\delta_\tau(z); \mathbf{V}) - \overline{L}_D(\delta_\tau(z); \mathbf{V})) \right) = \frac{1}{\sqrt{n}} \sum_{i=1}^n \zeta_{ni}. \end{aligned}$$

As ζ_{ni} forms a triangular array of martingale differences with respect to the σ -fields $(\mathfrak{F}_{i-1})_i$, we are now able to apply the central limit theorem under the unconditional Lindeberg condition (see [30]). More precisely, we need to verify the following condition:

$$\frac{1}{n} \sum_{i=1}^n \mathbb{E}[\zeta_{ni}^2 | F_{i-1}] \rightarrow 1 \quad \text{in probability}$$

and

$$\text{for every } \epsilon > 0 \quad \frac{1}{n} \sum_{i=1}^n \mathbb{E}[\zeta_{ni}^2 \mathbb{1}_{\zeta_{ni}^2 > \epsilon n}] \rightarrow 0. \quad (27)$$

The first one is obtained by standard analytical arguments in functional statistics. While for (27), we use the fact that

$$\zeta_{ni}^2 \mathbb{1}_{\zeta_{ni}^2 > \epsilon n} \leq \frac{|\zeta_{ni}|^{2+c}}{\sqrt{(\epsilon n)^c}} \quad \text{for every } c > 0$$

to prove that

$$\frac{1}{n} \sum_{i=1}^n \mathbb{E}[\zeta_{ni}^2 \mathbb{1}_{\zeta_{ni}^2 > \epsilon n}] \rightarrow 0.$$

□